

## 2. Theory

### 1) Relationship between total magnetic moment and total angular momentum

Strictly speaking, the total magnetic moment of an atom consists of electron magnetic moment and nuclear magnetic moment while the former is three orders of magnitude larger than the latter. As a result, only the electron magnetic moment is considered here. The orbital motion of an electron in an atom creates orbital magnetic moment, while the spin motion of an electron results in spin magnetic moment.

Based on quantum mechanics, the numerical relationship between the orbital magnetic moment  $\mu_L$  and the orbital angular momentum  $P_L$  of an electron is as follows:

$$\mu_L = \frac{e}{2m} P_L \quad \text{with } P_L = \sqrt{L(L+1)}\eta \quad (1)$$

The relationship between the spin magnetic moment  $\mu_S$  and the spin angular momentum  $P_S$  is as follows:

$$\mu_S = \frac{e}{m} P_S \quad \text{with } P_S = \sqrt{S(S+1)}\eta \quad (2)$$

where  $e$  and  $m$  are the charge and mass of an electron, respectively;  $L$  and  $S$  are the orbital quantum number and spin quantum number, respectively. The total angular momentum of the atom  $P_J$  is the sum of orbital angular momentum and spin angular momentum while the total magnetic moment  $\mu$  is the sum of orbital magnetic moment and spin magnetic moment. Since  $\mu$  moves around  $P_J$ , the net projection of  $\mu$  on  $P_J$  is not zero, i.e.  $\mu_J \neq 0$ . The numerical relationship between  $\mu_J$  and  $P_J$  is written as:

$$\mu_J = g \frac{e}{2m} P_J \quad (3)$$

where

$$g = 1 + \frac{J(J+1) - L(L+1) + S(S+1)}{2J(J+1)} \quad (4)$$

is the Lande  $g$ -factor that determines the energy-level splitting amount in a magnetic field.

### 2) Effect of external magnetic field on atomic energy levels

In an external magnetic field, the introduced torque  $L$  on the total magnetic moment  $\mu$  of an atom is:

$$L = \mu_J \times B, \quad (5)$$

where  $B$  is the magnetic induction. Torque  $L$  forces angular momentum  $P_J$  moving around the magnetic field direction. This motion brings additional energy:

$$\Delta E = -\mu_J B \cos \alpha. \quad (6)$$

Substituting (3) into (6), one can get:

$$\Delta E = g \frac{e}{2m} P_J B \cos \alpha . \quad (7)$$

Since the orientations of  $\boldsymbol{\mu}_J$  and  $\boldsymbol{P}_J$  are quantized in a magnetic field, i.e. the components of  $\boldsymbol{P}_J$  are quantized in the direction of the magnetic field, and it must be an integer times of  $\eta$ , that is,

$$P_J \cos \alpha = M\eta \quad M = J, (J-1), \dots, -J \quad (8)$$

There are totally  $2J+1$  magnetic quantum numbers. Substituting (8) into (7), we get:

$$\Delta E = Mg \frac{e\eta}{2m} B . \quad (9)$$

Thus, one energy level is split into  $2J+1$  sub-levels in an external magnetic field with the additional energy of each sub-level determined by (9), which is proportional to the product of the external magnetic field  $B$  and the Lande  $g$ -factor.

### 3) Selection rules of the Zeeman effect

If a spectral line is emitted by electron transition from energy level  $E_2$  to energy level  $E_1$  in the absence of an external magnetic field, the frequency  $\nu$  of this spectral line is given by

$$h\nu = E_2 - E_1 . \quad (10)$$

In the presence of an external magnetic field, the upper and lower energy levels are split into  $2J_2+1$  and  $2J_1+1$  sub energy levels with additional energies  $\Delta E_2$  and  $\Delta E_1$ , respectively. The frequency of the new spectral line  $\nu'$  is given by:

$$h\nu' = (E_2 + \Delta E_2) - (E_1 + \Delta E_1) . \quad (11)$$

Therefore, the frequency difference between the spectral lines is:

$$\Delta\nu = \nu' - \nu = \frac{1}{h}(\Delta E_2 - \Delta E_1) = (M_2 g_2 - M_1 g_1) \frac{eB}{4\pi m} . \quad (12)$$

When represented by wave number, (12) can be rewritten as:

$$\Delta\tilde{\nu} = (M_2 g_2 - M_1 g_1) \frac{eB}{4\pi mc} . \quad (13)$$

The Lorentz unit  $L = eB/(4\pi mc) = 4.67 \times 10^{-3} \text{ Bm}^{-1}$ , where  $B$  is in unit of  $G_s$  ( $1 G_s = 10^{-4} \text{ T}$ ).

It should be pointed out that not any transitions between any two energy levels are permitted. Transitions must meet selection rules as:  $\Delta M = M_2 - M_1 = 0, \pm 1$  with an exception of  $M_2 = 0 \rightarrow M_1 = 0$  when  $J_2 = J_1$ .

(1) when  $\Delta M = 0$ ,  $\pi$  lines are generated with linear polarization parallel to the magnetic field when observing along the direction perpendicular to the magnetic field. When observing along the magnetic field, light intensity is zero.

(2) when  $\Delta M = \pm 1$ ,  $\sigma^\pm$  lines are generated with linear polarization perpendicular to the magnetic field when observing along the direction perpendicular to the magnetic field. When the propagation direction of light is along the direction of the magnetic field,  $\sigma^+$  line is a left-

handed circularly polarized light while  $\sigma^-$  line is a right-handed circularly polarized light; when the propagation direction of light is  $180^\circ$  of the direction of magnetic field, the observed  $\sigma^+$  and  $\sigma^-$  lines are right-handed and left-handed circularly polarized light, respectively; when observed in other directions,  $\pi$  lines still remain as linearly polarized light, but  $\sigma$  lines become circularly polarized light. Since the light source must be placed between the two magnetic poles of a magnet, a hole must be opened on each pole in order to observe the Zeeman effect along the magnetic field direction.

#### 4) Zeeman effect of Mercury green line

The Mercury green line used in this experiment is at 546.1 nm corresponding to transitions between energy levels  $6s7s^3S_1 \rightarrow 6s6p^3P_2$  with the corresponding quantum numbers,  $g$ ,  $M$ ,  $Mg$ , and polarization states listed in Tables 1 and 2.

Table 1 Polarization states of spectral lines

Selection rules	$K \perp B$ (transverse)	$K \parallel B$ (longitudinal)
$\Delta M = 0$	Linearly polarized $\pi$ component	No light
$\Delta M = +1$	Linearly polarized $\sigma$ component	right-handed circularly polarized
$\Delta M = -1$	Linearly polarized $\sigma$ component	left-handed circularly polarized

Where  $K$  is the optical wave vector,  $B$  is the magnetic induction vector,  $\sigma$  represents vector  $E \perp B$ , and  $\pi$  represents vector  $E \parallel B$ .

Table 2 Energy levels with corresponding quantum numbers

Atomic states	$7^3S_1$	$6^3P_2$
L	0	1
S	1	1
J	1	2
g	2	3/2
M	1, 0, -1	2, 1, 0, -1, -2
Mg	2, 0, -2	3, 3/2, 0, -3/2, -3

The Lande factor  $g$  and the splitting of the two atomic states in a magnetic field can be calculated by (4) and (7), and the transition diagram can be plotted as shown in Figure 1.

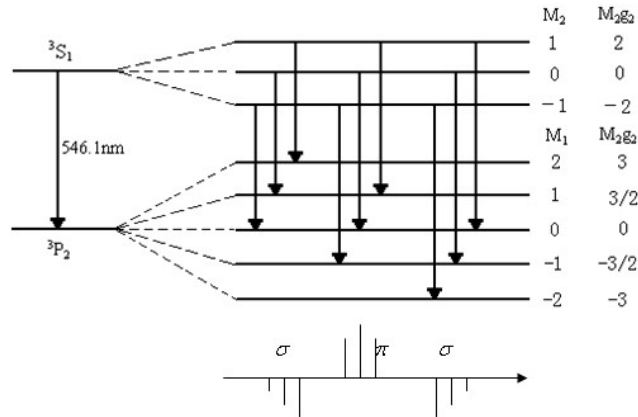


Figure 1 Zeeman effect and intensity distribution of Mercury green line

As seen in Figure 1, the upper and lower energy levels are split into 3 and 5 sub levels in an external magnetic field, respectively. The allowed nine transitions by selection rules are shown in the diagram. The appropriate spectral locations of the spectral lines are drawn at the bottom of the energy level diagram with the wave number increasing from left to right equidistantly. The heights of these line segments represent the relative intensities of the actual spectral lines.

### 5) Theory of Fabry-Perot etalon

As the wavelength difference of Zeeman splitting is very small, a regular prism or grating does not have enough resolution to separate these spectral lines. In this experiment, a Fabry-Perot etalon is used to resolve Zeeman spectral line separations. The principle of an etalon is as follows. When a ray of light passes through a plane-parallel plate with two reflecting surfaces, it is reflected many times between the two surfaces and hence multiple-beam interference occurs. The higher the surface reflectance is, the sharper the interference fringes are. As shown in Fig. 2, two partially reflecting mirrors  $G_1$  and  $G_2$  are aligned parallel to each other, forming a reflective cavity. When monochromatic light is incident on the reflective cavity with an angle  $\theta$ , many parallel rays pass through the cavity to get transmitted. The optical path difference between two neighboring rays is given by  $\delta$ , as:

$$\delta = 2nd \cos \theta, \quad (14)$$

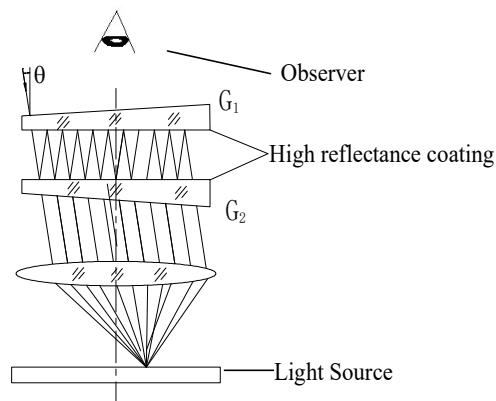


Figure 2 Schematic of Fabry-Perot interferometer

where  $n$  is the refractive index of the medium in the cavity,  $d$  is the cavity length or mirror spacing, and  $\lambda$  is the wavelength of the monochromatic light in vacuum. Thus, the transmitted light intensity is:

$$I' = I_0 \frac{1}{1 + \frac{4R}{(1-R)^2} \sin^2 \frac{\pi\delta}{\lambda}}, \quad (15)$$

where  $I_0$  is the incident light intensity,  $R$  is the mirror reflectance.

Thus,  $I'$  varies with  $\delta$ . When

$$2nd \cos \theta = K\lambda. \quad (K = 0, 1, 2, \dots) \quad (16)$$

$I'$  becomes maximum so that constructive interference of the transmitted light occurs.

Since the interference of an etalon is multiple-beam interference, the width of interference pattern becomes very fine (sharp). Usually, the resolution of an etalon is represented by the parameter of finesse  $F$ :

$$F = \frac{\pi\sqrt{R}}{1-R}. \quad (17)$$

Considering two monochromatic light beams at wavelengths  $\lambda_1$  and  $\lambda_2$  with a small wavelength separation ( $\lambda_1 > \lambda_2$  and  $\lambda_1 \cong \lambda_2 \cong \lambda$ ), e.g. the split light beams of a Mercury green line by Zeeman effect. For the same order of the interference  $m$ , as described in (16), the intensity Maxima of  $\lambda_1$  and  $\lambda_2$  correspond to different incident angles  $\theta_1$  and  $\theta_2$ , forming two sets of interference patterns.

By increasing the wavelength separation (i.e. increasing magnetic field intensity), so that the  $K^{\text{th}}$  order maximum of  $\lambda_2$  overlaps with the  $(K-1)^{\text{th}}$  order maximum of  $\lambda_1$ , as

$$K\lambda_2 = (K-1)\lambda_1. \quad (18)$$

Under paraxial conditions ( $\theta \cong 0$ ), (16) can be rewritten as  $K=2nd/\lambda$ , thus (18) becomes as:

$$\Delta\lambda = \lambda_1 - \lambda_2 = \frac{\lambda^2}{2nd}. \quad (19)$$

Represented by wave number, (19) becomes:

$$\Delta\tilde{\nu} = 1/(2nd). \quad (20)$$

The calculated  $\Delta\lambda$  or  $\Delta\tilde{\nu}$  based on (19) or (20) is called the free spectral range of the etalon.

The gap of an etalon can be solid or air. An air-gap etalon consists of two pieces of high reflection coated mirrors which are in parallel configured with a specific gap by using proper adjustment mechanism, while a solid-gap etalon is a single piece of optical material, and the parallelism of the two surfaces is already ensured during the production process that there is no need to adjust the parallelism in experiment.

## 6) Measurement of wavelength separation

Image the interference pattern of an etalon to the focal plane of a lens with focal length  $f$ , as

seen in Fig. 3. The relationship between incident angle  $\theta$  and diameter  $D$  of an interference ring at the central portion of the pattern can be written as:

$$\cos \theta = \frac{f}{\sqrt{f^2 + (D/2)^2}} \approx 1 - \frac{1}{8} \frac{D^2}{f^2}. \quad (21)$$

Substitute (21) into (16), we get:

$$2nd \left( 1 - \frac{D^2}{8f^2} \right) = K\lambda. \quad (22)$$

It is apparent from (22) that the square of the diameter of a fringe in central portion has a linear relationship with the order of the interference  $K$ . The fringes at a fixed wavelength get denser with an increase in fringe diameter. Further, a larger diameter fringe corresponds to a lower order of the interference. Similarly, for the same order of the interference, a larger diameter fringe corresponds to a smaller wavelength.

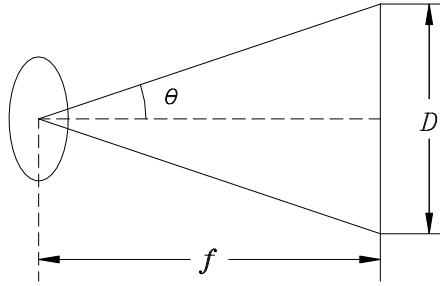


Figure 3 Relationship between incident angle and fringe diameter

The difference between the squares of diameters of adjacent orders of the interference  $K$  and  $K-1$  at same wavelength can be derived from (22), as:

$$\Delta D^2 = D_{K-1}^2 - D_K^2 = \frac{4f^2\lambda}{nd}. \quad (23)$$

Obviously,  $\Delta D^2$  is a constant, independent of the order of the interference.

Similarly, the wavelength difference of fringes at the same order of the interference  $K$  can be calculated from (22). For example, the wavelength difference between two adjacent spectral lines from Zeeman splitting can be written as:

$$\lambda_a - \lambda_b = \frac{d}{4f^2K} (D_b^2 - D_a^2) = \frac{\lambda}{K} \frac{D_b^2 - D_a^2}{D_{K-1}^2 - D_K^2}. \quad (24)$$

Because the order of the interference  $K$  is normally near the central portion,  $K \approx 2d/\lambda$ . (24) can be rewritten as:

$$\lambda_a - \lambda_b = \frac{\lambda^2}{2nd} \frac{D_b^2 - D_a^2}{D_{K-1}^2 - D_K^2}. \quad (25)$$

Or in wave number:

$$\vartheta'_a - \vartheta'_b = \frac{1}{2nd} \frac{D_b^2 - D_a^2}{D_{K-1}^2 - D_K^2} = \frac{1}{2nd} \frac{\Delta D_{ab}^2}{\Delta D^2}. \quad (26)$$

Substituting (26) into (13), we get the charge-mass ratio of an electron:

$$\frac{e}{m} = \frac{2\pi \cdot c}{(M_2 g_2 - M_1 g_1) B n d} \left( \frac{D_b^2 - D_a^2}{D_{K-1}^2 - D_K^2} \right). \quad (27)$$